HHS Public Access

Author manuscript

Arch Pharm Res. Author manuscript; available in PMC 2017 September 08.

Published in final edited form as:

Arch Pharm Res. 2016 July ; 39(7): 897–911. doi:10.1007/s12272-016-0784-y.

New ursane triterpenoids from *Ficus pandurata* and their binding affinity for human cannabinoid and opioid receptors

Amgad I. M. Khedr[1], **Sabrin R. M. Ibrahim**[2,3], **Gamal A. Mohamed**[4,5], **Hany E. A. Ahmed**[2,6], **Amany S. Ahmad**[3], **Mahmoud A. Ramadan**[3], **Atef E. Abd El-Baky**[7], **Koji Yamada**[8], and **Samir A. Ross**[9]

[1]Department of Pharmacognosy, Faculty of Pharmacy, Port Said University, Port Said 42526, Egypt

[2]Department of Pharmacognosy and Pharmaceutical Chemistry, College of Pharmacy, Taibah University, Al Madinah Al Munawarah 30078, Saudi Arabia

[3]Department of Pharmacognosy, Faculty of Pharmacy, Assuit University, Assuit 71526, Egypt

[4]Department of Natural Products and Alternative Medicine, Faculty of Pharmacy, King Abdulaziz University, Jeddah 21589, Saudi Arabia

[5]Department of Pharmacognosy, Faculty of Pharmacy, Al-Azhar University, Assuit Branch, Assuit 71524, Egypt

[6]Pharmaceutical Organic Chemistry Department, Faculty of Pharmacy, Al-Azhar University, Cairo, Egypt

[7]Department of Biochemistry, Faculty of Pharmacy, Port Said University, Port Said 42526, Egypt

[8]Garden for Medicinal Plants, Graduate School of Biomedical Sciences, Nagasaki University, Bunkyo-machi 1-14, Nagasaki 852-8521, Japan

[9]National Center for Natural Products Research, and Department of Pharmacognosy, School of Pharmacy, University of Mississippi, University, MS 38677, USA

Abstract

Phytochemical investigation of *Ficus pandurata* Hance (Moraceae) fruits has led to the isolation of two new triterpenoids, ficupanduratin A [1β-hydroxy-3β-acetoxy-11α-methoxy-urs-12-ene] (**11**) and ficupanduratin B [21α-hydroxy-3β-acetoxy-11α-methoxy-urs-12-ene] (**17**), along with 20 known compounds: α-amyrin acetate (**1**), α-amyrin (**2**), 3β-acetoxy-20-taraxasten-22-one (**3**), 3β-acetoxy-11α-methoxy-olean-12-ene (**4**), 3β-acetoxy-11α-methoxy-12-ursene (**5**), 11-oxo-α-amyrin acetate (**6**), 11-oxo-β-amyrin acetate (**7**), palmitic acid (**8**), stigmast-4,22-diene-3,6-dione (**9**), stigmast-4-ene-3,6-dione (**10**), stigmasterol (**12**), β-sitosterol (**13**), stigmast-22-ene-3,6-dione (**14**), stigmastane-3,6-dione (**15**), 3β,21β-dihydroxy-11α-methoxy-olean-12-ene (**16**), 3β-hydroxy-11α-methoxyurs-12-ene (**18**), 6-hydroxystigmast-4,22-diene-3-one (**19**), 6-hydroxystigmast-4-ene-3-one (**20**), 11α,21α-dihydroxy-3β-acetoxy-urs-12-ene (**21**), and β-

Correspondence to: Sabrin R. M. Ibrahim.

Compliance with ethical standards

Conflict of interest The authors report no conflicts of interest with respect to this work.

sitosterol-3-*O*-*β*-D-glucopyranoside (**22**). Compound **21** is reported for the first time from a natural source. The structures of the **20** compounds were elucidated on the basis of IR, 1D (^{1}H and ^{13}C), 2D (^{1}H–^{1}H COSY, HSQC, HMBC and NOESY) NMR and MS spectroscopic data, in addition to comparison with literature data. The isolated compounds were evaluated for their anti-microbial, anti-malarial, anti-leishmanial, and cytotoxic activities. In addition, their radioligand displacement affinity on opioid and cannabinoid receptors was assessed. Compounds **4**, **11**, and **15** exhibited good affinity towards the CB2 receptor, with displacement values of 69.7, 62.5 and 86.5 %, respectively. Furthermore, the binding mode of the active compounds in the active site of the CB2 cannabinoid receptors was investigated through molecular modelling.

Keywords

Ficus pandurata; Triterpenes; Cannabinoid receptors; Opioid receptors; Anti-malarial; Anti-leishmanial

Introduction

Medicinal plants have been used extensively as a source of numerous active constituents for treating human diseases and have a high therapeutic value (Nostro et al. 2000). *Ficus* (Moraceae), which comprises more than 800 species, is a large genus of trees or shrubs cultivated for their ornamental leaves and edible fruits (Metcalf and Chalk 1950; Baily 1963; Lin and Wunder 1997). Plants of the *Ficus* genus are distributed in tropical and subtropical regions (Mbosso et al. 2012) and known to be rich sources of triterpenes and sterols (Tuyen et al. 1998; Kuo and Chiang 1999; Ragasa et al. 1999; Chiang et al. 2001; Chiang and Kuo 2001, 2002; Kuo and Lin 2004; Chiang et al. 2005; Sisy and Abeba 2005; Parveen et al. 2009). In Ayurvedic and traditional Chinese medicine (TCM), *Ficus* species are widely used for the treatment of various diseases such as inflammation, diabetes, tumour and malaria (Singh et al. 2011). In Egypt, many *Ficus* species are found in streets, gardens and parks, as well as outside canal banks (Harborne 1973; Riffle 1998). The fruits of *F. carica* L. and *F. sycomorus* L. are two of the most popular fruits eaten by Egyptians. In traditional Egyptian medicine, *Ficus* species are used for anti-diabetic, hypotensive and anti-cough applications, as well as in the treatment of respiratory disorders and certain skin diseases (Chopra et al. 1950; Edlin and Nimmo 1978; Mousa et al. 1994). Large quantities of latex, which is a source of rubber, have been found in the wood of *Ficus* species, representing one of the largest economical uses of *Ficus* in Egypt (Edlin and Nimmo 1978). *F. pandurata* Hance, known as Xiao xianggou in Lishui District (Zhejiang, China), can be used for removing dampness and strengthening the spleen. It is also used in TCM to treat gout, arthritis, hyperuricemia, and indigestion (Chen et al. 2005; Lei and Li 2007). To the best of our knowledge, there are few reports about the phytochemical composition and biological activities of *F. pandurata* (Jeong and Lachance 2001; Basudan et al. 2005; Vaya and Mahmood 2006; Zhang et al. 2015). Our previous phytochemical study of *F. pandurata* led to the isolation of sterols and triterpenes (Ramadan et al. 2009; Ahmed 2010; Khedr et al. 2015). As a continuation of our investigation, we report herein the isolation and structural elucidation of two new triterpenes, ficupanduratins A (**11**) and B (**17**), along with 20 known compounds from the fruit of *F. pandurata* H (Fig. 1). The structures of these compounds

were verified by various spectroscopic methods. The anti-microbial, anti-malarial, anti-leishmanial, and cytotoxic activities of the isolated compounds were evaluated. In addition, their radioligand displacement affinity on opioid and cannabinoid receptors has been tested.

Materials and methods

General experimental procedures

Optical rotations were measured with a JASCO DIP-370 digital polarimeter. Melting points were determined using an Electrothermal 9100 Digital Melting Point apparatus (Electrothermal Engineering Ltd., Essex, England). IR spectra were obtained using a JASCO FT/IR-410 spectrophotometer. HRFABMS were recorded on a JMS DX-303 spectrometer (JEOL Ltd., Japan) using *m*-nitrobenzyl alcohol or Magic Bullet as a matrix. HRESIMS were measured on a Finnigan MAT 95 mass spectrometer. ESIMS were recorded on a Finnigan MAT TSQ-7000 triple stage quadrupole mass spectrometer. EIMS were recorded on a JEOL JMS-SX/SX 102A mass spectrometer. 1D and 2D NMR spectra were recorded with a Unity Plus 500 spectrometer (Varian Inc., USA) operating at 500 MHz for ^{1}H and 125 MHz for ^{13}C. ^{1}H NMR chemical shifts are expressed in δ values referring to the solvent peak of δ_H 7.26 for $CDCl_3$ and δ_H 7.19, 7.55 and 8.71 for C_5D_5N; coupling constants are expressed in Hz. ^{13}C NMR chemical shifts are expressed in δ values referring to the solvent peaks δ_C 77.23 for $CDCl_3$ and δ_C 123.5, 135.5 and 149.9 for C_5D_5N. Sephadex LH-20 (0.25–0.1 mm, Pharmacia Fine Chemical Co. Ltd, Piscataway, NJ), Wakogel C-300 (Wako Pure Chemical Industries, Ltd, Japan, 45–75 μm) and Cosmosil 5C18-140 PREP (Nacalai Tesque, No. 379-34) were used for column chromatography. Pre-coated Kieselgel 60 F_{254} silica gel plates (0.25 mm, Merck, Darmstadt, Germany) and RP-18 F_{254s} plates (0.04–0.063 mm, Merck, Darmstadt, Germany) were used for thin-layer chromatographic analysis. Semi-preparative HPLC was performed on a Develosil C30-UG-5 column (250 × 4.6 mm, Nomura Chemical Co., Aichi, Japan) and a Wakosil-II 5sil-100 column (150 × 4.6 mm ‘B’, Wako Pure Chemical Industries Ltd., Japan) at a flow rate of 1.5 mL/min, equipped with a TOSOH RI-8020 detector and a JASCO BIP-I HPLC pump.

Plant material

Fruits of *F. pandurata* were collected in May 2013 from authorized trees growing in the garden of the Faculty of Pharmacy, Assiut University. The plant was taxonomically identified by Prof. Dr. Salah EL-Nagar (Professor of Botany, Department of Botany, Faculty of Science, Assiut University, Egypt). A voucher specimen (registration code FPF-2013) was deposited at the Department of Pharmacognosy, Faculty of Pharmacy, Al-Azhar University, Assiut, Egypt.

Extraction and isolation

The air-dried and powdered fruits (1.1 kg) were exhaustively extracted by cold percolation with 70 % MeOH (4 × 4 L) at room temperature. The alcoholic extract was concentrated under vacuum to afford a dark brown residue (95 g). The residue was mixed with 500 mL distilled H_2O and subjected to solvent fractionation using EtOAc and *n*-BuOH; the fractions were separately concentrated to yield EtOAc (37 g), *n*-BuOH (21 g) and aqueous (28 g) extracts. The EtOAc extract was subjected to vacuum liquid chromatography (VLC) using *n*-

hexane:EtOAc and EtOAc:MeOH gradient to give 20 fractions (F1–F20). Fraction F1 (3.4 g, 5 % EtOAc/*n*-hexane) was subjected to silica gel column chromatography (*n*-hexane:EtOAc 10:0 to 9:1), yielding eight sub-fractions (A–H). Sub-fraction F1-B (360 mg) was subjected to semi-preparative HPLC (Wakosil-II 5sil-100) using 100 % MeOH to give compounds **1** (R_t 55 min, 125 mg, white needles) and **2** (R_t 43 min, 160 mg, white amorphous powder). Semi-preparative HPLC (Wakosil-II 5sil-100) using 100 % MeOH of sub-fraction F1-F (295 mg) gave **3** (R_t 14 min, 20 mg, white needles), **4** (R_t 23 min, 50 mg, white amorphous solid) and **5** (R_t 34 min, 78 mg, white amorphous solid). Sub-fraction F1-H (95 mg) was chromatographed by semi-preparative HPLC (Develosil C-30-UG-5) using 100 % MeOH to yield **6** (R_t 22 min, 12 mg, colourless amorphous solid) and 7 (R_t 38 min, 8 mg, colourless amorphous solid). Fraction F3 (1.6 g) eluted by 15 % EtOAc/*n*-hexane was chromatographed over silica gel CC using *n*-hexane:EtOAc gradient to yield four sub-fractions (A–D). Sub-fraction F3-A (348 mg) was subjected to ODS CC (95 % MeOH:H_2O) to give compound **8** (127 mg, white amorphous solid) and three sub-fractions (A1–A3). Sub-fraction F3-A3 (53 mg) was subjected to semi-preparative HPLC (Develosil C-30-UG-5) using MeOH:H_2O (95:5) to afford **9** (R_t 35 min, 16 mg, pale yellow amorphous solid) and **10** (R_t 31 min, 31 mg, pale yellow amorphous solid). Sub-fraction F3-B (479 mg) was chromatographed on silica gel CC using *n*-hexane:EtOAc gradient to yield four sub-fractions (B1–B4). Sub-fraction F3-B2 (300 mg) was subjected to ODS CC (95 % MeOH:H_2O) to yield three sub-fractions (B2a–B2c). Sub-fraction F3-B2a (43 mg) was subjected to semi-preparative HPLC (Develosil C-30-UG-5) using MeOH:H_2O (95:5) to give **11** (R_t 48 min, 5 mg, white amorphous powder). Sub-fraction F3-B2c (250 mg) was subjected to semi-preparative HPLC (Wakosil-II 5sil-100) using 100 % MeOH to obtain **12** (R_t 54 min, 232 mg, colourless amorphous solid) and **13** (R_t 60 min, 27 mg, colourless amorphous solid). ODS column chromatography (90 % MeOH:H_2O) of sub-fraction F3-D (300 mg) yielded four sub-fractions (D1–D4). Semi-preparative HPLC (Wakosil-II 5sil-100) using 95 % MeOH of sub-fractions F3–D3 (27 mg) and F3–D4 (53 mg) gave **14** (R_t 48 min, 13 mg, colourless amorphous solid, F3–D3), **15** (R_t 52 min, 5.8 mg, colourless amorphous solid, F3 to D3), **16** (R_t 58 min, 19 mg, colourless amorphous solid, F3–D4), **17** (R_t 65 min, 5 mg, white amorphous powder, F3–D4) and **18** (R_t 73 min, 7 mg, colourless amorphous solid, F3–D4). Fraction F5 (0.78 g, 30 % EtOAc/*n*-hexane) was chromatographed over silica gel CC using *n*-hexane:EtOAc gradient to yield four sub-fractions (A–D). Sub-fraction F5-B (300 mg) was chromatographed on Sephadex LH-20 ($CHCl_3$:MeOH; 1:1) to yield three sub-fractions (B1–B3). Sub-fraction F5–B2 (23 mg) was subjected to semi-preparative HPLC (Wakosil-II 5sil-100) using 100 % MeOH to give **19** (R_t 83 min, 9.8 mg, colourless amorphous solid) and **20** (R_t 87 min, 7.8 mg, colourless amorphous solid). Sub-fraction F5-C (80 mg) was crystallized from MeOH to obtain impure **21**, which was further purified on Sephadex LH-20 ($CHCl_3$:-MeOH; 1:1) to yield **21** (7 mg, white needles). Compound **22** (350 mg, white amorphous powder) was crystallized from fraction F9 (0.95 g, *n*-hexane:EtOAc 95:5) by MeOH.

Ficupanduratin A (**11**): White amorphous powder (5 mg). m.p. 139–141 °C (dec.) $[\alpha]_D^{25}+51.3$ (*c* 0.87 $CHCl_3$). IR (KBr) ν_{max} 3458, 2943, 1732, 1618, 1046 cm^{-1}. NMR data: see Tables 1 and 2. HRESIMS *m*/*z* 537.3916 (calcd for $C_{33}H_{54}NaO_4$, 537.3920 $[M + Na]^+$) and 1051.7939 (calcd for $C_{66}H_{108}NaO_8$, 1051.7942 $[2M + Na]^+$).

Ficupanduratin B (**17**): White amorphous powder (5 mg). 143–145 C (dec.) $[\alpha]_D^{25}+66.4$ (*c* 0.15, $CHCl_3$). IR (KBr) ν_{max} 3478, 2955, 1725, 1454, 1032, 665 cm^{-1}. NMR data: see Tables 1 and 2. HRFABMS *m*/*z* 515.4106 (calcd for $C_{33}H_{55}O_4$, 515.4100 $[M + H]^+$), 483.3873 $[M + H\text{-}OCH_3]^+$.

11α,21α-dihydroxy-3β-acetoxy-urs-12-ene (**21**): White needles (7.0 mg). m.p. 261–263 °C. $[\alpha]_D^{25}+45.7$ (*c* 0.87, $CHCl_3$); IR (KBr) ν_{max} 3425, 2950, 1725, 1630, 1450, 1320, 1015 cm^{-1}; NMR data: see Tables 1 and 2; HRFABMS *m*/*z* 501.3946 (calcd for $C_{32}H_{53}O_4$, $[M + H]^+$, 501.3944).

Radioligand displacement for cannabinoid and opioid receptor subtypes

Compounds **1**–**22** were evaluated in competition binding with cannabinoid receptor subtypes, cannabinoid receptor 1 (CB1) and cannabinoid receptor 2 (CB2), as previously described (Thomas et al. 2005; León et al. 2013). Also, these compounds were tested against the opioid receptor subtypes (*δ*, *κ* and *μ*) as previously described (León et al. 2013).

Assays

Anti-microbial assay—All the isolated compounds were tested for their anti-microbial activity at concentrations of 20-0.8 μg/mL against *Candida albicans* ATCC 90028, *Candida glabrata* ATCC90030, *Candida krusei* ATCC 6258, *Asperigillus fumigates* ATCC 90906, methicillin-resistant *Staphylococcus aureus* ATCC 33591, *Cryptococcus neoformans* ATCC 90113, *Staphylococcus aureus* ATCC 2921, *Escherichia coli* ATCC 35218, *Klebsiella pneumonia* ATCC 13883, *Pseudomonus aeruginosa* ATCC 27853 and *Mycobacterium intracellulare* ATCC 23068 using modified versions of the CLSI/NCCLS methods (Ibrahim et al. 2012a, 2015a, b).

Anti-malarial assay—The isolated compounds were tested at concentrations of 4760–528.9 ng/mL on chloroquine sensitive (D6, Sierra Leone) and resistant (W2, Indochina) strains of *Plasmodium falciparum*. Standard anti-malarial agents, chloroquine and artemisinin, were used as positive controls, whereas DMSO was used as a negative control (El-Shanawany et al. 2011; Ibrahim et al. 2016; Elkhayat et al. 2016).

Anti-leishmanial assay—The anti-leishmanial activity of the isolated metabolites was tested in vitro against *L. donovani* promastigotes as previously described (Ibrahim et al. 2012a, 2015a, b). Pentamidine and amphoterecin B were used as positive controls.

Cytotoxicity assay—The in vitro cytotoxic activity of the compounds was determined against noncancerous kidney cell lines (VERO) at concentrations of 4760-528.9 ng/mL. The cell line was obtained from the American Type Culture Collection (ATCC, Rockville, MD). The cell viability was determined using Neutral Red dye according to a previous method with modification (Borenfreund et al. 1990; Mohamed et al. 2013; Ibrahim et al. 2015a, b). Doxorubicin was used as a positive control, whereas DMSO was used as the negative control.

Molecular modelling and docking studies

Receptor modelling—The Homology Modelling module implemented in the program Molecular Operation Environment (MOE, version 2010.11, Chemical Computing Group Inc., Montreal, Canada) was employed to build the CB2 model (MOE 2012). For this purpose, the sequence of human CB2 was subjected to a protein database (PDB) search (Munro et al. 1993; Liu et al. 2007) of the protein structure database implemented in MOE 2010.11 with the Z cutoff set to 2.0 while leaving the other parameters at their default values. The search suggested the human adenosine receptor A2a (hAA2R) as a template for the comparative modelling procedure on the basis of high similarity, and the hAA2R structure [PDB:3EML] was chosen as the reference for the sequence alignment. After downloading the 3D structure of [PDB:3QAK] from the RCSB database (Liu et al. 2007), the structure was superimposed on the crystal structure of hAA2R. After removal of all lipid molecules, ions and water molecules, the residues between 209 and 222, which belong to lysozyme T4, were removed from the structure. In order to improve the modelling accuracy, the co-crystallized agonist UK-432097 of [PDB:3QAK] was retained in the system during the modelling procedure. Ten independently generated models were generated employing the default parameters of the homology modelling module, and only the consensus model was computed. An energy-minimization step was applied for the optimization of the new protein model; this aided the removal of residue clashes using the AMBER89 force field with default values. The quality of the model was verified by running the Protein Report module of MOE. After removal of the template ligand UK-432097, the primary structure receptor was energy minimized to convergence, giving the final hCB2 model structure.

Compounds docking studies—Small compounds were built in MOE with subsequent geometry optimization based on the MMFF force field incorporated in the program package, with a distance-dependent dielectric constant. The residues of the proposed binding pocket were defined based on the Site Finder module of MOE. The same binding site was proposed in the literature (Abood 2005). For the molecular docking studies, the module dock in MOE with parameters set to their default values was employed. All single bonds of the small ligands were allowed to rotate freely during the docking simulation. The side chains of the residues composing the binding pocket were treated as flexible, and the atoms of the protein backbone were maintained at fixed positions. The predicted poses were analysed according to their low energy states and were selected for presentation.

Results

The dried fruits of *Ficus pandurata* were extracted with MeOH. The concentrated MeOH extract was mixed with H_2O and partitioned between EtOAc and *n*-BuOH. The EtOAc extract was subjected to VLC, silica gel, Sephadex LH-20, ODS, and semi-preparative HPLC column chromatography to yield two new (**11** and **17**) and 20 known compounds (**1**–**10**, **15**, **16**, and **18**–**22**).

Compound **11** was obtained as white amorphous powder. It gave a positive Liebermann-Burchard reaction (Gołembiewska et al. 2013; Al Musayeib et al. 2014), indicating its triterpenoidal nature. Its molecular formula was determined as $C_{33}H_{54}O_4$ based on the

HRESIMS pseudo-molecular ion peaks at *m*/*z* 537.3916 (calcd for $C_{33}H_{54}NaO_4$, 537.3920 $[M+Na]^+$) and 1051.7939 (calcd for $C_{66}H_{108}NaO_8$, 1051.7942 $[2M+Na]^+$), requiring 7° of unsaturation. These degrees of unsaturation can be accounted for by five ring systems, one olefinic double bond, and one acetoxy carbonyl group. The HRESIMS showed characteristic fragment ion peaks at *m*/*z* 467.4360 $[M+H–(OCH_3+OH)]^+$ and 424.3731 $[M+H–(OCH_3+–OH+COCH_3)]^+$. Its IR spectrum showed characteristic absorption bands for hydroxyl (3458 cm^{-1}), acetoxy (1732 cm^{-1}) and double bonds (1618 cm^{-1}). The ^{13}C and HSQC spectra showed the presence of 33 carbons, comprising 10 methyls, 7 methylenes, 9 methines (3 for oxymethines at δ_C 76.8 (C-1), 76.2 (C-3) and 73.0 (C-11) and 1 for a *tri*-substituted olefinic double bond at δ_C 122.0 (C-12)), and 7 quaternary carbons, including one for a carbonyl carbon at δ_C 170.7 (C-31). Detailed 1D and 2D NMR analysis of **11** suggested that it is an ursane-type pentacyclic triterpene (Ibrahim et al. 2012b). The ^1H NMR spectrum of **11** exhibited six singlet methyls at δ_H 0.95 (H_3-23), 0.88 (H_3-24), 1.07 (H_3-25), 1.02 (H_3-26), 1.16 (H_3-27) and 0.82 (H_3-28) and two doublet methyl groups at δ_H 0.84 (d, *J* = 6.5 Hz, H_3-29) and 0.97 (d, *J* = 6.5 Hz, H_3-30), supporting the ursane-type carbon framework of **11** (Mahato and Kundu 1994; Ibrahim et al. 2012b). They correlated to the carbons resonating at δ_C 27.9, 16.3, 18.1, 18.0, 22.6, 28.9, 17.4 and 21.2, respectively, in the HSQC spectrum. In the HMBC spectrum, H_3-23 and H_3-24 showed cross peaks to C-3, C-4 and C-5; H_3-25 to C-5, C-9 and C-10; H_3-26 to C-7, C-8, C-9 and C-14; H_3-27 to C-8, C-13, C-14 and C-15; H_3-28 to C-16, C-17 and C-18; H_3-29 to C-18, C-19 and C-20; and H_3-30 to C-19, C-20 and C-21, confirming their positions. Moreover, the ^1H and ^{13}C NMR spectra of **11** revealed signals at δ_C 5.45 (d, *J* = 4.0 Hz, H-12) and δ_C 122.0 (C-12) and 145.4 (C-13), indicating the presence of a tri-substituted olefinic double bond. The double bond was established at C-12/C-13 from the HMBC correlations of H_3-27 to C-13 and H-9 and H-18 to C-12 (Fig. 2). Three oxymethine groups were observed at δ_H 3.53 (dd, *J* = 11.5, 5.0 Hz, H-1), 5.06 (dd, *J* = 12.0, 4.5 Hz, H-3) and 3.74 (dd, *J* = 8.5, 4.0 Hz, H-11), correlating to the carbon signals at δ_C 76.8 (C-1), 76.2 (C-3) and 73.0 (C-11) in the HSQC spectrum. This assignment was secured by the ^1H–^1H COSY correlations of 1-OH (δ_H 4.35) and H-2 with H-1 and H-3, as well as H-9 and H-12 with H-11; it was also confirmed by the HMBC cross peaks of 1-OH, H-3, H-9 and H_3-25 to C-1; H-5, H_3-23 and H_3-24 to C-3; and H-9 and H-12 to C-11 (Fig. 2). Additionally, the signals at δ_H 2.03 (H_3-32)/δ_C 21.5 (C-32) and 170.7 (C-31) indicated the presence of an acetoxy group in **11**. This was further confirmed by the IR absorption band at 1732 cm^{-1} and further secured by the ESIMS fragment ion peak at *m*/*z* 473 $[M+H–COCH_3]^+$. Its connectivity at C-3 was established on the basis of the HMBC correlation of H-3 to C-31 and confirmed by the downfield shift of H-3 (δ_H 5.06). Furthermore, a methoxy group was observed at δ_H 3.37 (11-OCH_3)/δ_C 55.8 (11-OCH_3). Its HMBC cross peak to C-11 established its placement at C-11. The relative stereochemistry at C-1, C-3 and C-11 was assigned based on the comparison of the ^1H and ^{13}C chemical shifts as well as the coupling constant values with those of related triterpenes; it was confirmed by the NOESY experiment (Topçu and Ulubelen 1999; Mathias et al. 2000; Chiang and Kuo 2001; Mallavadhani et al. 2006; Mohamed 2014). The NOESY cross peaks of H-1 to H-3, H-5 and H-9 as well as H-9 to 11-OCH_3, H_3-27 and H_3-30 indicated that these protons were present on the same side of the molecule. Furthermore, the correlations of H-11 with H-18, H_3-25 and H_3-26 and H-20 with H-18 and H_3-28 suggested that these protons are on the other side of the molecule. On the basis of these findings and by comparison with the literature

(Mahato and Kundu 1994; Mathias et al. 2000), the structure of **11** was assigned as 1β-hydroxy-3β-ace-toxy-11α-methoxy-urs-12-ene. To the best of our knowledge, **11** is a new triterpenoid, to which the name ficupanduratin A was given.

Compound **17** was obtained as a white amorphous powder. The HRFABMS showed a pseudo-molecular ion peak at *m*/*z* 515.4106 (calcd for $C_{33}H_{55}O_4$, 515.4100 $[M+H]^+$), corresponding to a molecular formula of $C_{33}H_{54}O_4$. The IR, ^1H and ^{13}C NMR spectral data of **17** were similar to those of **11**, with the exception that the signals for the oxymethine group at δ_H 3.53 (dd, *J* = 11.5, 5.0 Hz, H-1)/δ_C 76.8 (C-1) and the methylene groups at δ_H 2.10 (m, H-2A) and 1.95 (m, H-2B)/δ_C 32.2 (C-1) were missing. Instead, a new signal at δ_H 3.45 (ddd, *J* = 10.0, 3.0, 3.0 Hz, H-21) correlated to the methine proton at δ_H 1.34 (m, H-20) and the methylene proton at δ_H 1.43 (m, H-22) in the ^1H–^1H COSY spectrum, indicating the presence of an oxymethine group at C-21. This was confirmed by the HMBC cross peaks of H-30 [δ_H 0.88 (d, *J* = 6.5 Hz)] and H-19 to C-21 (Topçu et al. 2003). The β-configuration of H-21 was assigned based on the coupling constant value and was confirmed by the observed NOESY correlations of H-21 with H-18 and H-28 (Topçu et al. 2003). Based on the data obtained from the COSY, HSQC, HMBC and NOESY experiments, the structure of **17** was identified as 21α-hydroxy-3β-acetoxy-11α-methoxy-urs-12-ene; this compound was named ficupanduratin B.

Compound **21** was obtained as white needles. The molecular formula was $C_{32}H_{52}O_4$, confirmed by the HRFABMS pseudo-molecular ion peak at *m*/*z* 501.3946 $[M + H]^+$ (calcd for $C_{32}H_{53}O_4$, 501.3944). Compound **21** was 15 mass units less than **17**, suggesting that **21** had one methyl group less than **17**. The ^1H and ^{13}C NMR spectra (Tables 1, 2) of **21** were almost identical to those of **17**; however, the signals associated with the methoxy group at δ_H 3.36 (11-OCH_3)/δ_C 53.5 (11-OCH_3) in **17** were absent. The NMR data of **21** were identical to those of 11α,21α-dihydroxy-3β-acetoxy-urs-12-ene, which was previously obtained synthetically (Topçu et al. 2003). This is the first report of its isolation from a natural source. On the basis of the coupling constant values and NOESY correlations, the configuration of **21** was assigned to be the same as that of **17** and of 11α,21α-dihydroxy-3β-acetoxy-urs-12-ene.

The known compounds were identified by analysing the spectroscopic data (1D and 2D NMR) and comparing their data with those in the literature to be α-amyrin acetate (**1**) (Virgilio et al. 2015), α-amyrin (**2**) (Virgilio et al. 2015), 3β-acetoxy-20-taraxasten-22-one (**3**) (Ramadan et al. 2009; Ahmed 2010), 3β-acetoxy-11α-methoxy-olean-12-ene (**4**) (Kuo and Chiang 2000; Mallavadhani et al. 2006; Barbosa et al. 2010), 3β-acetoxy-11α-methoxy-12-ursene (**5**) (Mathias et al. 2000; Barbosa et al. 2010), 11-oxo-α-amyrin acetate (**6**) (Fingolo et al. 2013), 11-oxo-β-amyrin acetate (**7**) (Fingolo et al. 2013), palmitic acid (**8**) (Ajoku et al. 2015), stigmast-4,22-diene-3,6-dione (**9**) (Itokawa et al. 1973), stigmast-4-ene-3,6-dione (**10**), stigmasterol (**12**) (Mohamed and Ibrahim 2007; Kamboj and Salujai 2011; Chaturvedula and Prakash 2012), β-sitosterol (**13**) (Al-Musayeib et al. 2013), stigmast-22-ene-3,6-dione (**14**) (Wei et al. 2004), stigmastane-3,6-dione (**15**) (Wei et al. 2004; Lim et al. 2005), 3β,21β-dihydroxy-11α-methoxy-olean-12-ene (**16**) (Cáceres-Castillo et al. 2008), 3β-hydroxy-11α-methoxyurs-12-ene (**18**) (Fujita et al. 2000), 6-

hydroxystigmast-4,22-diene-3-one (**19**) (Kontiza et al. 2006; Georges et al. 2006), 6-hydroxystigmast-4-ene-3-one (**20**) (Kontiza et al. 2006; Georges et al. 2006) and *β*-sitosterol-3-*O*-*β*-D-glucopyranoside (**22**) (Khatun et al. 2012).

The isolated compounds **1**–**22** were evaluated for their anti-microbial activity against *C. albicans*, *C. glabrata*, *C. krusei*, *A. fumigates*, methicillin-resistant *S. aureus* (MRSA), *C. neoformans*, *S. aureus*, *E. coli*, *P. aeruginosa* and *M. intracellulare*; their anti-leishmanial activity against *L. donovani* promastigotes; and their anti-malarial activity against chloroquine-sensitive (D6, Sierra Leone) and resistant (W2, Indochina) strains of *Plasmodium falciparum*. Furthermore, they were tested for cytotoxicity against the VERO cell line. The results showed that none of the tested compounds had activity in these assays.

In addition, these compounds were evaluated using in vitro radioligand binding affinity assays of cannabinoid receptors (CB1 and CB2) and opioid receptors (subtypes δ, κ and μ) as described previously (León et al. 2013; Thomas et al. 2005). It is noteworthy that compounds **4**, **11**, and **15** (conc. 10 μM) selectively inhibited 69.7, 62.5 and 86.6 %, respectively, of the specific binding of [^{3}H]-CP-55,940 to human embryonic kidney (HEK) cell membranes expressing human CB2 (Fig. 3; Table 3). Meanwhile, compound **6** exhibited low radioligand binding displacement at 10 μM, with an affinity of 22.2 % for the CB2 receptor. Moreover, compounds **4**, **8**, **13**, **14**, **15**, **16**, **19**, and **22** showed moderate inhibition, with affinity values of 36.9, 39.1, 24.9, 44.5, 44.4, 22.4, 22.8 and 32.2 %, respectively, of the specific binding of [^{3}H]-CP-55,940 to HEK cell membranes expressing human CB1. Interestingly, only compounds **6** and **22** inhibited 22.8 and 21.2 % of the specific binding [^{3}H]-DPDPE to HEKhDOR cell membranes expressing *δ*-opioid receptors at 10 μM, respectively. Compounds **8**, **12**, **13**, **17**, and **21** displaced the U-69,593 radioligand to HEKhKOR cell membranes expressing *κ*-opioid receptors by 22.1, 36.1, 28.1, 30.9 and 26.5 %, respectively. However, compounds **6** and **20** inhibited 23 and 28.5 % of the specific binding of [^{3}H]-DAMGO to HEKhMOR cell membranes expressing *μ*-opioid receptors, respectively.

Molecular modelling studies were performed to obtain a more detailed structure-based analysis of the binding mode of the most active compounds towards CB2. For the CB receptors, no experimentally determined crystal structures are yet available. Hence, a homology modelling protocol was used to build a three-dimensional (3D) structure model of this receptor. Sequence similarity searches were performed to establish this protocol, and the results obtained identified the human beta1-adrenergic receptor (bAR1) [PDB:2Y00] (Warne et al. 2011) as the closest structure with the highest sequence similarity to the hCB2 sequence. However, the X-ray structure of the human A2A adenosine receptor ([PDB: 3QAK]) was selected as the template for comparative modelling (Xu et al. 2011). The newly constructed 3D model of human CB2 with the proposed binding pocket is shown in Fig. 4. Moreover, a mutagenesis protocol was applied in the binding pocket residues of reference ligand CP-55,940 (a CB1/CB2 cannabinoid receptor agonist) so that these residues are accessible in the new proposed model (Poso and Huffman 2008). This model was in agreement with published work (Rühl et al. 2012).

In order to investigate the productivity as well as the characteristics of the binding site of our models and to facilitate structure–activity relationship (SAR) analysis of the active cannabinoid receptor ligands **4**, **11** and **15**, docking analysis was performed on the reference CP-550,940 to adjust the structures of the residues (Fig. 5). Analysis of the receptor-ligand complex models generated after successful ligand docking was based on the analysis of hydrogen bonding interactions, aromatic and hydrophobic interactions, and binding energy (Table 4). The placement of ligands in the proposed pocket revealed different types of interactions, including three hydrogen bonding interactions with Lys109, Ser285 and Ala282 residues with distances ranging between 1.9 and 2.5 Å through the compound side chains. In addition, the alkyl side chain exhibited tolerably stable hydrophobic aromatic interactions with corresponding Val251, Met265 and Leu254 amino acids. However, **4**, **11**, and **15** showed mostly similar binding modes of interaction to the reference ligand, mainly with Ser285, Lys279 and Ala282, through the formation of stable hydrogen bonds. The most prominent feature in these compounds is their greater rigidity, which orients the structures to fit in the CB2 binding pocket. Also, molecular descriptors were calculated for all compounds, including descriptions of their polarity, lipophilicity and solubility, as structural indicators for topological and surface analyses (Table 5).

Discussion

Both natural and synthetic triterpenoids have a wide range of unique and potentially biological activities, including anti-microbial, antioxidant, anti-inflammatory, hepato-and cardioprotective, anticancer, anti-HIV, antiulcerogenic, antiplasmodial, and analgesic activities (Dzubak et al. 2006; Laszczyk 2009; Vrao and Patlolla 2012; Zhang et al. 2013; Han and Bakovic 2015). Vitor et al. (2009) and Okoye et al. (2014) reported that α-amyrin acetate (**1**) and α-amyrin (**2**) exhibited pronounced anti-inflammatory effects and suppressed the levels of inflammatory cytokines and COX-2 levels via inhibition of NF-κB activity and of signalling pathways involving phospho-cyclic AMP response element binding protein (Vitor et al. 2009; Okoye et al. 2014). Moreover, **2** inhibited platelet aggregation induced by adenosine 5′-diphosphate, collagen and arachidonic acid (Aragão et al. 2007). Qi et al. 2008 mentioned that stigmast-4,22-diene-3,6-dione (**9**) exhibited anti-larval activity. Compounds **12** and **13** possessed anti-inflammatory activity through inhibition of cytokines, prostaglandin E2, lipoxgenase-5 and cyclooxygenase-2 (Prieto et al. 2006; Al-Attas et al. 2015). Also, **12** and **13** showed effective anti-genotoxic activity (Lim et al. 2005).

To the best of our knowledge, this is the first report of the evaluation of the affinity of this class of compounds towards human cannabinoid and opioid receptors. The cannabinoid and opioid receptors are G-protein coupled receptors and have long been known to modulate pain (Bushlin et al. 2010). Natural compounds with selective affinity for specific opioid and cannabinoid receptors could provide novel drug leads for neuropathic pain (Gao et al. 2013). Special interest has been focused in CB2 as a target for the treatment of neuropathic pain, inflammatory conditions and a variety of other pathologies (Grimsey et al. 2011). It is noteworthy that compounds **4**, **11**, and **15** showed good selective CB2 receptor binding affinity. The results confirmed that these compounds can be considered as lead structures for novel CB2 selective ligands. This is one of the possible mechanisms of the anti-inflammatory effect of triterpenoids. Hence, **4**, **11**, and **15** could represent potential anti-

inflammatory compounds. This supports the rationale behind the traditional use of this plant in the treatment of inflammation and its related symptoms.

Acknowledgments

We are grateful to Mr. M. Inada, Mr. N. Yam-aguchi and Mr. N. Tsuda of the Scientific Support Section of Joint Research Center, Nagasaki University, for ^{1}H NMR, ^{13}C NMR and MS measurements. This work was supported in part by a Grant-in-Aid for Scientific Research [Grant Number 23590008 and 26460124] from the Japan Society for the Promotion of Science, which is gratefully acknowledged. The in vitro binding assay using opioid and cannabinoid receptors was made possible by a grant from the NIGMS, a component of the National Institutes of Health (NIH) [Grant Number P20GM104932]. The contents of this work are solely the responsibility of the authors and do not necessarily represent the official views of NIGMS or NIH.

References

Abood ME. Molecular biology of cannabinoid receptors. Handbook Exp Pharmacol. 2005; 168:81–115.

Ahmed AS. Pentacyclic triterpenes from *Ficus pandurata* Hance fruit. Bull Pharm Sci Assiut Univ. 2010; 33:1–7.

Ajoku GA, Okwute SK, Okogun JI. Isolation of hexadecanoic acid methyl ester and 1,1,2-ethanetricarboxylic acid-1-hydroxy-1, 1-dimethyl ester from the calyx of Green *Hibiscus Sabdariffa* (Linn). Nat Prod Chem Res. 2015; 3:1–5.

Al Musayeib NM, Mothana RA, Ibrahim SRM, El Gamal AA, Al-Massarani SM. Klodorone A and klodorol A: new triterpenes from *Kleinia odora*. Nat Prod Res. 2014; 28:1142–1146. [PubMed: 24831019]

Al-Attas AAM, El-Shaer NS, Mohamed GA, Ibrahim SRM, Esmat A. Anti-inflammatory sesquiterpenes from *Costus speciosus* rhizomes. J Ethnopharmacol. 2015; 176:365–374. [PubMed: 26593213]

Al-Musayeib NM, Mohamed GA, Ibrahim SRM, Ross SA. lupeol-3-o-decanoate, a new triterpene ester from *Cadaba farinosa* forsk. growing in Saudi Arabia. Med Chem Res. 2013; 22:5297–5302.

Aragão GF, Carneiro LMV, Júnior APF, Bandeira PN, Lemos TLG, Viana GSB. Antiplatelet activity of α- and β-amyrin, isomeric mixture from *Protium heptaphyllum*. Pharm Biol. 2007; 45:343–349.

Baily, LH. The standard cyclopedia of horticulture. 11. The MacMillan Co; New York: 1963. p. 1229-1233.

Barbosa LF, Mathias L, Braz-Filho R, Curcino Vieira IJ. Chemical constituents from *Aspidosperma illustre* (Apocynaceae). J Braz Chem Soc. 2010; 21:1434–1438.

Basudan OA, Ilyas M, Parveen M, Muhisen HMH, Kumar R. A new chromone from *Ficus lyrata*. J Asian Nat Prod Res. 2005; 7:81–85. [PubMed: 15621607]

Borenfreund E, Babich H, Martin-Alguacil N. Rapid chemosensitivity assay with human normal and tumor cells in vitro. In Vitro Cell Dev Biol. 1990; 26:1030–1034. [PubMed: 2177465]

Bushlin I, Rozenfeld R, Devi LA. Cannabinoid-opioid interactions during neuropathic pain and analgesia. Curr Opin Pharmacol. 2010; 10:80–86. [PubMed: 19857996]

Cáceres-Castillo D, Mena-Rejón GJ, Cedillo-Rivera R, Quijano L. 21β-hydroxy-oleanane-type triterpenes from *Hippocratea excels*. Phytochemistry. 2008; 69:1057–1064. [PubMed: 18061220]

Chaturvedula VSP, Prakash I. Isolation of stigmasterol and β-sitosterol from the dichloromethane extract of Rubus suavissimus. Int Curr Pharm J. 2012; 1:239–242.

Chen, SF., Lu, GZ., Zhao, WL. Traditional chinese medicine processing standards of zhejiang province. Zhejiang Science and Technology Press; Hangzhou: 2005.

Chiang YM, Kuo YH. New peroxy triterpenes from the aerial roots of *Ficus microcarpa*. J Nat Prod. 2001; 64:436–439. [PubMed: 11325223]

Chiang YM, Kuo YHY. Novel triterpenoids from the aerial roots of *Ficus microcarpa*. J Org Chem. 2002; 67(7656–7661):22. [PubMed: 11777434]

Chiang YM, Su KJ, Liu YH, Kuo YH. New cyclopropyltriterpenoids from the aerial roots of *Ficus microcarpa*. Chem Pharm Bull. 2001; 49:581–583. [PubMed: 11383610]

Chiang YM, Chang JY, Kuo CC, Chang CY, Kuo YH. Cytotoxic triterpenes from the aerial roots of *Ficus microcarpa*. Phytochemistry. 2005; 66:495–501. [PubMed: 15694457]

Chopra, RN., Chubra, IC., Handa, RL., Kapin, LD. Indigenous drugs of India. U.N. Dhur and Sons Private Ltd; Calcutta: 1950.

Dzubak P, Hajduch M, Vydra D, Hustova A, Kvasnica M, Biedermann D, Markova L, Urban M, Sarek J. Pharmacological activities of natural triterpenoids and their therapeutic implications. Nat Prod Rep. 2006; 23:394–411. [PubMed: 16741586]

Edlin, H., Nimmo, M. The illustrated encyclopedia of trees: timbers and forests of the world. Salamander; London: 1978. p. 220-221.

Elkhayat ES, Ibrahim SRM, Mohamed GA, Ross SA. Terrenolide S, a new anti-leishmanial butenolide from the endophytic fungus *Aspergillus terreus*. Nat Prod Res. 2016; 30:814–820. [PubMed: 26299734]

El-Shanawany MA, Ross SA, Ibrahim SRM, Mohamed GA, Nafady AM. A new xanthone from the roots of *Centaurium spicatum* L. Phytochem Lett. 2011; 4:126–128.

Fingolo CE, Santos TS, Vianna Filho MDM, Kaplan MAC. Triterpene eEsters: natural products from *Dorstenia arifolia* (Moraceae). Molecules. 2013; 18:4247–4256. [PubMed: 23579992]

Fujita R, Duan H, Takaishi Y. Terpenoids from tripterigyum hypoglaucum. Phytochemistry. 2000; 53:715–722. [PubMed: 10746886]

Gao J, Radwan MM, León F, Dale OR, Husni AS, Wu Y, Lupien S, Wang X, Manly SP, Hill RA, Dugan FM, Cutler HG, Cutler SJ. *Neocosmospora* sp.-derived resorcylic acid lactones with in vitro binding affinity for human opioid and cannabinoids receptors. J Nat Prod. 2013; 76(5):824–828. [PubMed: 23659286]

Georges P, Sylvestre M, Ruegger H, Bourgeois P. Ketosteroids and hydroxyketosteroids, minor metabolites of sugarcane wax. Steroids. 2006; 71:647–652. [PubMed: 16797622]

Gołembiewska E, Skalicka-WoŸniak K, Głowniak K. Methods for the isolation and identification of triterpenes and sterols in medicinal plants. Curr Issues Pharm Med Sci. 2013; 26:26–32.

Grimsey NL, Goodfellow CE, Dragunow M, Glass M. Cannabinoid receptor 2 undergoes Rab5-mediated internalization and recycles via a Rab11-dependent pathway. Biochim Biophys Acta. 2011; 1813:1554–1560. [PubMed: 21640764]

Han N, Bakovic M. Biologically active triterpenoids and their cardioprotective and anti-inflammatory effects. J Bioanal Biomed S. 2015; 12:005.doi: 10.4172/1948-5

Harborne, JB. Phytochemical methods: a guide to modern techniques of plant analysis. Champan and Hall; London: 1973. p. 221-232.

Ibrahim SRM, Mohamed GA, Al-Musayeib NM. New constituents from the rhizomes of Egyptian *Iris germanica* L. Molecules. 2012a; 17:2587–2598. [PubMed: 22388969]

Ibrahim SRM, Mohamed GA, Shaala LA, Banuls LMY, Van Goietsenoven G, Kiss R, Youssef DTA. New ursane type triterpenes from the root bark of *Calotropis procera*. Phytochem Lett. 2012b; 5:490–495.

Ibrahim SRM, Elkhayat ES, Mohamed GA, Khedr AIM, Fouad MA, Kotb MHR, Ross SA. Aspernolides F and G, new butyrolactones from the endophytic fungus *Aspergillus terreus*. Phytochemistry Lett. 2015a; 14:84–90.

Ibrahim SRM, Mohamed GA, Moharram AM, Youssef DTA. Aegyptolidines A and B: new pyrrolidine alkaloids from the fungus *Aspergillus aegyptiacus*. Phytochem Lett. 2015b; 12:90–93.

Ibrahim SRM, Mohamed GA, Ross SA. Integracides F and G: new tetracyclic triterpenoids from the endophytic fungus *Fusarium sp*. Phytochem Lett. 2016; 15(24):125–130.

Itokawa H, Akasu M, Fugita M. Several oxidized sterols isolated from callus tissue of *Stephania cepharantha*. Chem Pharm Bull. 1973; 21:1386–1387.

Jeong WS, Lachance PA. Phytosterols and fatty acids in fig (*Ficus lyrata*, var. Mission) fruit and tree components. Food Chem Toxicol. 2001; 66:278–281.

Kamboj A, Salujai AK. Isolation of stigmasterol and βsitosterol from petroleum ether extract of aerial parts of *Ageratum conyzoides* (Asteraceae). Int. J Pharm Pharm Sci. 2011; 3:94–96.

Khatun M, Billah M, Abdul Quader M. Sterols and sterol glucoside from *Phyllanthus* species. Dhaka Univ J Sci. 2012; 60:5–10.

Khedr AIM, Nafady AM, Allam AE, Ahmed AS, Ramadan MA. Phytochemical and biological screening of the leaves of *Ficus pandurata* Hance cultivated in Egypt. J Pharm Phytochem. 2015; 4:50–54.

Kontiza I, Abatis D, Malakate K, Vagias C, Roussis V. 3-Keto steroids from the marine organism *Dendrophyllia cornigera* and *Cymodocea nodosa*. Steroids. 2006; 71:177–181. [PubMed: 16280145]

Kuo YH, Chiang YM. Five new taraxastane-type triterpenes from the aerial roots of *Ficus microcarpa*. Chem Pharm Bull. 1999; 47:498–500.

Kuo YH, Chiang YM. Six new ursane-and oleanane-type triterpenes from aerial roots of *Ficus microcarpa*. Chem Pharm Bull. 2000; 48:593–596. [PubMed: 10823690]

Kuo YH, Lin HY. Two novel triterpenes from the leaves of *Ficus microcarpa*. Helv Chim Acta. 2004; 87(5):1071–1076.

Laszczyk MN. Pentacyclic triterpenes of the lupane, oleanane and ursane group as tools in cancer therapy. Planta Med. 2009; 75:1549–1560. [PubMed: 19742422]

Lei, HX., Li, SF. Chinese Medicine of the 'She' Nationality. China Press of Traditional Chinese Medicine; Beijing: 2007.

León F, Gao J, Dale OR, Wu Y, Habib E, Husni AS, Hill RA, Cutler SJ. Secondary metabolites from Eupenicillium parvum and their in vitro binding affinity for human opioid and cannabinoid receptors. Planta Med. 2013; 79:1756–1761. [PubMed: 24288291]

Lim JC, Park JH, Budesinsky M, Kasal A, Han YH, Koo BS, Lee SI, Lee DU. Antimutagenic constituents from the thorns of *Gleditsia sinensis*. Chem Pharm Bull. 2005; 53:561–564. [PubMed: 15863930]

Lin, R., Wunder, P. Flora of North America. Oxford University press; New York: 1997. p. 388-389.p. 396-400.

Liu T, Lin Y, Wen X, Jorissen RN, Gilson MK. Binding DB: a web-accessible database of experimentally determined protein-ligand binding affinities. Nucleic Acids Res. 2007; 35:198–201.

Mahato SB, Kundu AP. 13C NMR spectra of pentacyclic triterpenoids: a compilation and some salient features. Phytochemistry. 1994; 37:1517–1575.

Mallavadhani UV, Narasimhan K, Sudhakar AVS, Mahapatra A, Li W, Breemen RBV. Three new pentacyclic triterpenes and some flavonoids from the fruits of an Indian ayurvedic plant dendrophthoe falcata and their estrogen receptor binding activity. Chem Pharm Bull. 2006; 54:740–744. [PubMed: 16651782]

Mathias L, Vieira IJC, Braz-Filho R, Filho ER. A new pentacyclic triterpene isolated from myroxylon balsamum (syn. Myroxylon peruiferum). J Braz Chem Soc. 2000; 11:195–198.

Mbosso EJT, Nguedia JCA, Meyer F, Lenta BN, Ngouela S, Lallemand B, Mathieu V, Van Antwerpen P, Njunda AL, Adiogo D, Tsamo E, Looze Y, Kiss R, Wintjens R. Ceramide, cerebroside and triterpenoid saponin from the bark of aerial roots of *Ficus elastica* (Moraceae). Phytochemistry. 2012; 83:95–103. [PubMed: 22963707]

Metcalf, CR., Chalk, L. Anatomy of dicotyledons. 11. The Clarendon Press; Oxford: 1950. p. 1259-1291.

MOE (The Molecular Operating Environment) Version. Chemical Computing Group Inc; 2012. http://www.chemcomp.com [Accessed 30 Feb 2013]

Mohamed GA. New cytotoxic cycloartane triterpene from *Cassia italica* aerial parts. Nat Prod Res. 2014; 28:976–983. [PubMed: 24684761]

Mohamed GA, Ibrahim SRM. Eucalyptone G, a new phloroglucinol derivative and other constituents from *Eucalyptus globulus* labill. ARKIVOC. 2007; 15:281–291.

Mohamed GA, Ibrahim SRM, Ross SA. New ceramides and isoflavone from the Egyptian Iris germanica L. rhizomes. Phytochem Lett. 2013; 6:340–344.

Mousa O, Vuorela P, Kiviranta J, Abdel Wahab S, Hiltunen R, Vuorel H. Bioactivity of certain Egyptian *Ficus* species. J Ethnopharmacol. 1994; 41:71–76. [PubMed: 8170162]

Munro S, Thomas KL, Abu-Shaar M. Molecular characterization of a peripheral receptor for cannabinoids. Nature. 1993; 365:61–65. [PubMed: 7689702]

Nostro A, Germano MP, D'Angelo V, Marino A, Cannatelli MA. Extraction methods and bioautography for evaluation of medicinal plant antimicrobial activity. Lett Appl Microbiol. 2000; 30:379–384. [PubMed: 10792667]

Okoye NN, Ajaghaku DL, Okeke HN, Ilodigwe EE, Nworu CS, Okoye FBC. Beta-amyrin and alpha-amyrin acetate isolated from the stem bark of *Alstonia boonei* display profound anti-inflammatory activity. Pharm Biol. 2014; 52:1478–1486. [PubMed: 25026352]

Parveen M, Ghalib RM, Mehdi SH, Rehman SZ, Ali M. A new triterpenoid from the leaves of *Ficus benjamina* (var. comosa). Nat Prod Res. 2009; 23:729–736. [PubMed: 19418356]

Poso A, Huffman JW. Targeting the cannabinoid CB2 receptor: modelling and structural determinants of CB2 selective ligands. Br J Pharmacol. 2008; 153:335–346. [PubMed: 17982473]

Prieto JM, Recio MC, Giner RM. Anti-inflammatory activity of beta-sitosterol in a model of oxazolone-induced contact delayed type hypersensitivity (in Spanish). Boletin Latinoamericano Y Del. 2006; 6:57–62.

Qi SH, Zhang S, Qian PY, Wang BG. Antifeedant, antibacterial, and antilarval compounds from the South China Sea seagrass *Enhalus acoroides*. Bot Mar. 2008; 51:441–447. DOI: 10.1515/BOT.2008.0XX

Ragasa CY, Juan E, Rideout JA. A triterpene from *Ficus pumzla*. J Asian Nat Prod Res. 1999; 1:269–275. [PubMed: 11523547]

Ramadan MA, Ahmad AS, Nafady AM, Mansour AI. Chemical composition of the stem bark and leaves of *Ficus pandurata* Hance. Nat Prod Res. 2009; 23:1218–1230. [PubMed: 19731141]

Riffle, RL. The tropical look. Thames and Hudson Ltd; London: 1998. p. 176-181.

Rühl T, Deuther-Conrad W, Fischer S, Günther R, Hennig L, Krautscheid H, Brust P. Cannabinoid receptor type 2 (CB2)-selective N-aryl-oxadiazolyl-propionamides: synthesis, radiolabelling, molecular modelling and biological evaluation. Org Med Chem Lett. 2012; 2:32.doi: 10.1186/2191-2858-2-32 [PubMed: 23067874]

Singh D, Singh B, Goel RK. Traditional uses, phytochemistry and pharmacology of *Ficus religiosa*: a review. J Ethnopharmacol. 2011; 134:565–583. [PubMed: 21296646]

Sisy F, Abeba B. Triterpene compounds from latex of Ficus sur. Bull Chem Soc Ethiopia. 2005; 19:307–310.

Thomas A, Stevenson LA, Wease KN, Price MR, Baillie G, Ross RA, Pertwee RG. Evidence that the plant cannabinoid D9-tetrahydrocannabivarin is a cannabinoid CB1 and CB2 receptor antagonist. Bri J Pharmacol. 2005; 146:917–926.

Topçu G, Ulubelen A. Terpenoids from *Salvia kronenburgii*. J Nat Prod. 1999; 62:1605–1608.

Topçu G, Altıner EN, Gözcü S, Halfon B, Aydoğmus Z, Pezzuto JM, Zhou BN, Kingston DGI. Studies on di- and triterpenoids from *Salvia staminea* with cytotoxic activity. Planta Med. 2003; 69:462–464. [PubMed: 12802731]

Tuyen NV, Kim DSHL, Fong HS, Soejarto DD, Khanh TC, Tri MV, Xuan LT. Structure elucidation of two triterpenoids from *Ficus fistulosa*. Phytochemistry. 1998; 50:467–469.

Vaya J, Mahmood S. Flavonoid content in leaf extracts of the fig (*Ficus lyrata* L.), carob (*Ceratonia siliqua* L.) and pistachio (*Pistacia lentiscus* L.). BioFactors. 2006; 28:169–175. [PubMed: 17473377]

Virgilio DE Jr, Shen C, Ragasa CY. Terpenoids and sterols from *Hoya multiflora* Blume. J Appl Pharm Sci. 2015; 5:33–39.

Vitor C, Figueiredo C, Hara D, Bento A, Mazzuco T, Calixto J. Therapeutic action and underlying mechanisms of a combination of two pentacyclic triterpenes, α-and β-amyrin, in a mouse model of colitis. Br J Pharmacol. 2009; 57:1034–1044.

Vrao C, Patlolla J. Triterpenoids for cancer prevention and treatment: current status and future prospects. Curr Pharm Biotechnol. 2012; 13:147–155. [PubMed: 21466427]

Warne T, Moukhametzianov R, Baker JG, Nehmé R, Edwards PC, Leslie AGW, Schertler GFX, Tate CG. The structural basis for agonist and partial agonist action on a β (1)-adrenergic receptor. Nature. 2011; 469:241–244. [PubMed: 21228877]

Wei K, Li W, Koiki K, Pei Y, Chen Y, Nikaido T. Spectral assignments and reference data: complete 1H and 13C NMR assignments of two phytosterols from roots of *Piper nigrum*. Magnet Reson Chem. 2004; 42:355–359.

Xu F, Wu H, Katritch V, Han GW, Jacobson KA, Gao ZG, Cherezov V, Stevens RC. Structure of an agonist-bound human A2A adenosine receptor. Science. 2011; 332:322–327. [PubMed: 21393508]

Zhang Y, Ning Z, Lu C, Zhao S, Wang J, Liu B, Xu X, Liu Y. Triterpenoid resinous metabolites from the genus *Boswellia*: pharmacological activities and potential species-identifying properties. Chem Cent J. 2013; 7:153.doi: 10.1186/1752-153X-7-153 [PubMed: 24028654]

Zhang XP, Lv HQ, Li ZG, Jiang KZ, Lee MR. HPLC/QTOF-MS/MS application to investigate phenolic constituents from *Ficus pandurata* H aerial roots. Biomed Chromatogr. 2015; 29:860–868. [PubMed: 25408477]

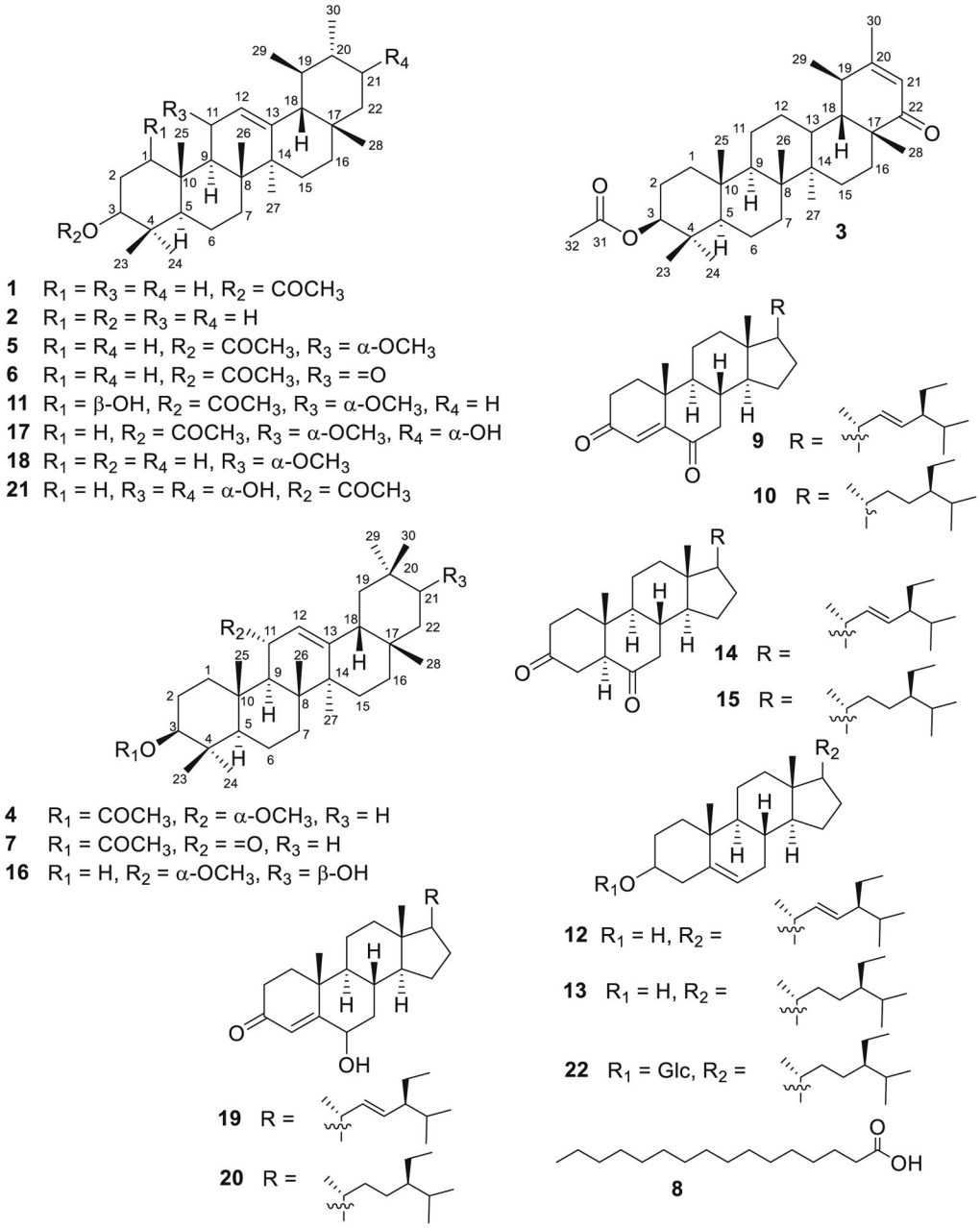

Fig. 1.
Structure of isolated compounds **1**–**22**

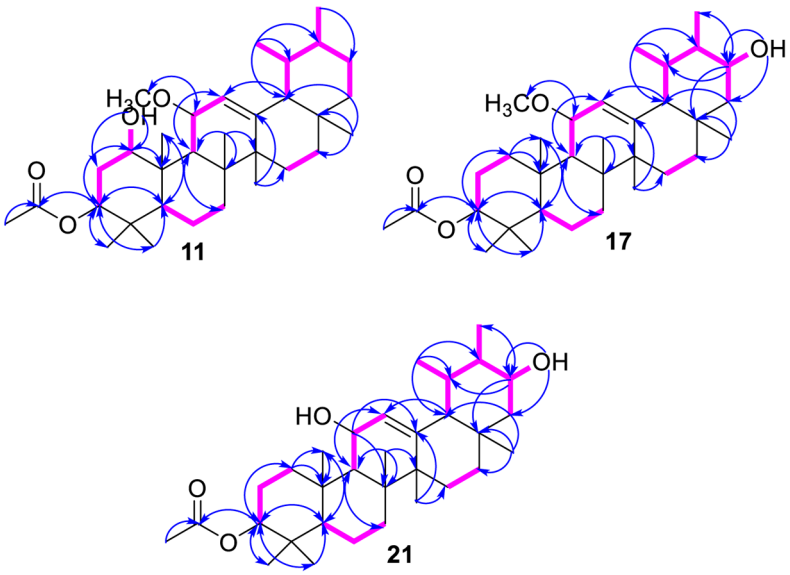

Fig. 2.
^{1}H–^{1}H COSY and HMBC correlations of **11**, **17** and **21**

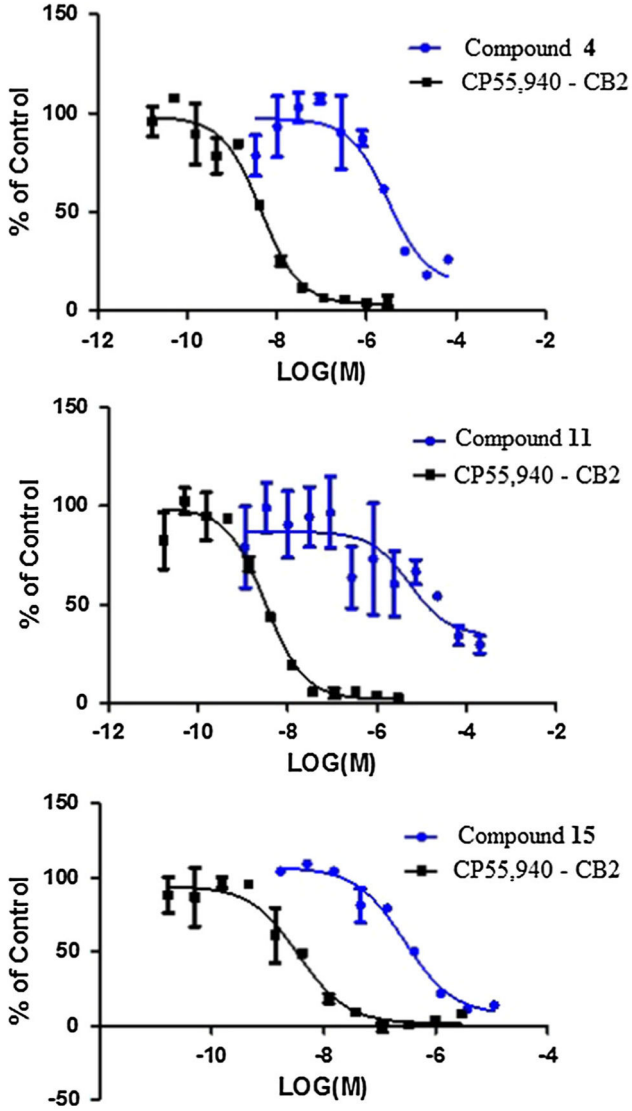

Fig. 3.

Displacement of [^{3}H]-CP55,940 binding by compounds **4**, **11**, and **15** in CB2 receptors

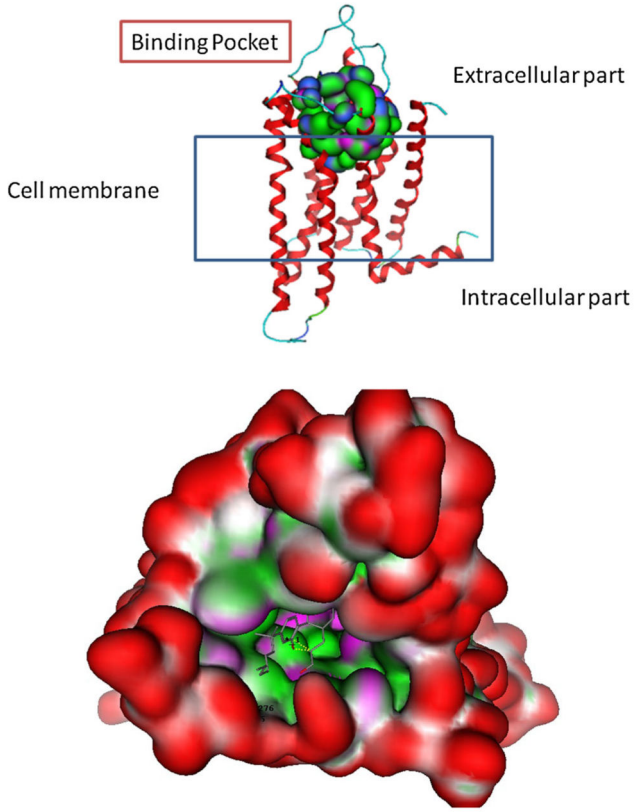

Fig. 4.

Molecular surface analysis of CB2 model. The protein is shown with the *N*-terminus at the top and the residues forming the binding pocket are shown in space-filling mode among the transmembrane helices and isolated figure as a surface with colour-coded features: H bonding (*magenta*), lipophilic (*green*), mild polar (*blue*)

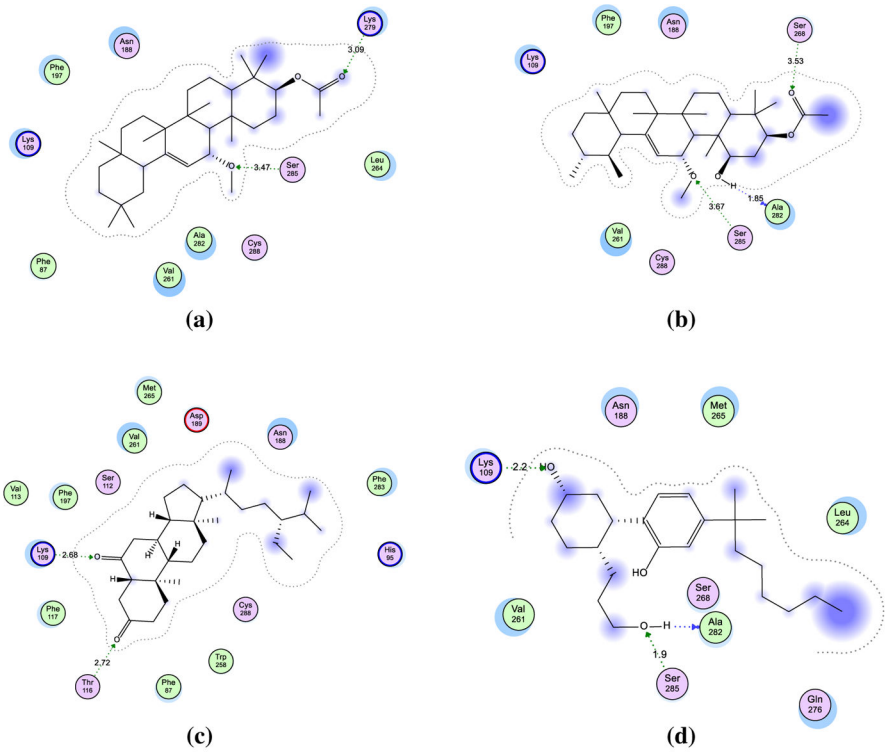

Fig. 5.

Hypothetical binding modes of the docked compounds **a 4**, **b 11**, **c 15**, and **d** CP-55,940 ligand. The figures exhibit the residues in the proposed binding pocket of CB2 model with corresponding hydrogen bonding interactions and hydrophobic contact

Table 1

1H NMR data of compounds **11**, **17**, and **21** (500 MHz, CDCl3)

Position	11	17	21
	δH, m, (*J* in Hz)	**δH, m, (*J* in Hz)**	**δH, m, (*J* in Hz)**
1	3.53 dd (11.5, 5.0)	1.86 m	1.48 m
		1.31 m	1.28 m
2	2.10 m	2.05 m	2.03 brdd (11.6, 4.5)
	1.95 m	2.00 m	1.98 m
3	5.06 dd (12.0, 4.5)	4.56 dd (12.0, 4.2)	4.56 dd (11.6, 4.5)
4	–	–	–
5	1.42 m	0.72 dd (10.0, 2.0)	0.73 brd (11.3)
6	1.65 m	1.38 m	1.38 m
	1.41 m	1.01 m	1.00 m
7	1.28 m	1.53 m	1.48 m
		0.87 m	1.31 m
8	–	–	–
9	2.27 d (8.5)	1.81 d (8.9)	1.68 d (9.2)
10	–	–	–
11	3.74 dd (8.5, 4.0)	4.13 dd (8.9, 3.5)	4.33 dd (9.4, 4.5)
12	5.45 d (4.0)	5.35 d (3.5)	5.23 d (4.0)
13	–	–	–
14	–	–	–
15	1.61 m	1.44 m	1.85 m
	1.21 m	0.89 m	1.78 m
16	1.52 m	1.41 m	1.38 m
		0.93 m	0.90 m
17	–	–	–
18	1.41 m	1.42 d (10.0)	1.41 m
19	1.36 m	0.95 m	0.87 m
20	0.96 m	1.34 m	1.34 m
21	1.32 m	3.45 ddd (10.0, 3.0, 3.0)	3.58 brdd (11.2, 2.5)
22	1.46 m	1.43 m	1.44 m
	1.31 m	1.28 m	1.30 m
23	0.95 s	0.86 s	0.87 s
24	0.88 s	1.05 s	1.10 s
25	1.07 s	0.87 s	0.87 s
26	1.02 s	1.08 s	1.04 s
27	1.16 s	1.15 s	1.16 s
28	0.82 s	0.80 s	0.80 s
29	0.84 d (6.5)	0.87 d (6.5)	0.88 d (6.4)
30	0.97 d (6.5)	0.88 d (6.5)	0.93 d (6.5)
1-OH	4.35 brs	–	–

Position	11	17	21
	δH, m, (*J* in Hz)	δH, m, (*J* in Hz)	δH, m, (*J* in Hz)
21-OH	–	6.13 d (3.0)	–
11-OCH3	3.37 s	3.36 s	–
31	–	–	–
32	2.03 s	2.06 s	2.06 s

Table 2

13C NMR and HMBC data of compounds **11**, **17**, and **21** (500 and 125 MHz, CDCl3)

Position	11		17		21	
	δC, *m*	**HMBC**	**δC, *m***	**HMBC**	**δC, *m***	**HMBC**
1	76.8 CH	3, 10	31.9 CH_2	3, 10, 25	31.0 CH_2	2, 3, 25
2	32.2 CH_2	3, 4, 10	27.8 CH_2	3, 4, 10	21.4 CH_2	4, 10
3	76.2 CH	1, 5, 23, 24, 31	77.3 CH	1, 5, 23, 24	77.6 CH	1, 2, 5, 23, 24
4	38.3 C	–	44.6 C	–	44.2 C	–
5	47.9 CH	3, 7, 10, 25	52.3 CH	3, 7, 23, 24, 25	52.3 CH	3, 10, 24, 25
6	18.3 CH_2	4, 6, 8	17.5 CH_2	7, 8	17.6 CH_2	5, 7, 8
7	31.3 CH_2	5, 9	33.3 CH_2	5, 6, 26	33.0 CH_2	5, 9, 26
8	42.0 C	–	43.8 C	–	43.7 C	–
9	45.9 CH	1, 7, 11, 12, 25, 26	51.8 CH	7, 11, 12, 25, 26	56.5 CH	7, 11, 12, 25, 26
10	43.0 C	–	38.0 C	–	37.8 C	–
11	73.0 CH	8, 9, 10, 12, 13, 11-OCH_3	77.0 CH	8, 10, 12, 13, 11-OCH_3	67.5 CH	8, 10, 12, 13, 11-OCH_3
12	122.0 CH	9, 11, 13, 14, 18, 27	122.5 CH	9, 11, 14, 18	126.5 CH	9, 11, 14, 18
13	145.4 C	–	146.2 C	–	144.4 C	–
14	42.5 C	–	41.9 C	–	41.9 C	–
15	27.1 CH_2	–	31.0 CH_2	8, 17	32.1 CH_2	8, 17
16	28.0 CH_2	–	27.1 CH2	14, 17, 28	26.9 CH_2	14, 17, 28
17	33.6 C	–	33.6 C	–	33.7 C	–
18	58.5 CH	–	58.6 CH	12, 16, 19, 29	57.8 CH	12, 16, 19, 29
19	39.5 CH	–	39.2 CH	13, 17, 21, 29	39.3 CH	13, 17, 21, 29
20	39.7 CH		39.4 CH	18, 22, 30	39.2 C	18, 22, 30
21	32.1 CH_2	–	76.7 CH	17, 19, 22, 30	76.7 CH	17, 19, 22, 30
22	41.5 CH_2	–	41.3 CH_2	17, 18, 20	41.2 CH_2	17, 18, 20
23	27.9 CH_3	3, 4, 5, 24	28.0 CH_3	3, 4, 5, 24	28.6 CH_3	3, 4, 5, 24
24	16.3 CH_3	3, 4, 5, 23	13.1 CH_3	3, 4, 5, 23	13.3 CH_3	3, 4, 5, 23
25	18.1 CH_3	1, 5, 9, 10	16.3 CH_3	1, 5, 9, 10	16.2 CH_3	1, 5, 9, 10
26	18.0 CH_3	7, 8, 9, 14	18.2 CH_3	8, 9, 14	17.9 CH_3	8, 9, 14

Position	11		17		21	
	δC, *m*	HMBC	δC, *m*	HMBC	δC, *m*	HMBC
27	22.6 CH_3	8, 13, 14, 15	22.4 CH_3	8, 13, 14, 15	23.1 CH_3	8, 13, 14, 15
28	28.9 CH_3	16, 17, 18	28.6 CH_3	16, 17, 18, 22	29.7 CH_3	16, 17, 18, 22
29	17.4 CH_3	18, 19, 20	17.7 CH_3	18, 19, 20	17.7 CH_3	18, 19, 20
30	21.2 CH3	19, 20, 21	21.4 CH_3	19, 20, 21	21.3 CH_3	19, 20, 21
1-OH	–	1, 2	–	–		–
21-OH			–	21, 22		21, 22
11-OCH3	55.8 CH_3	11	53.5 CH_3	11		11
31	170.7 C	–	170.8 C	–	170.8 C	–
32	21.5 CH_3	31	21.3 CH_3	31	21.4 CH_3	31

Table 3

Results of binding affinity assay of compounds **1**–**22** for human cannabinoid (subtypes CB1 and CB2) and opioid receptors (subtypes δ, κ, and μ)

Compounds	CB1 % Displacement	CB2 % Displacement	δ % Displacement	κ % Displacement	μ % Displacement
1	–	–	–	5.3	–
2	–	–	–	–	–
3	15.9	–	–	6.9	–
4	36.9	69.7	–	11.7	9.1
5	–	–	–	7.7	–
6	2.9	22.2	3.1	16.7	23
7	1.7	14.8	–	12.9	–
8	39.1	0.4	22.8	22.1	–
9	9.1	–	7.3	7.6	–
10	15.8	–	9.2	7.5	–
11	11.3	62.5	–	7	11.5
12	11.8	5.5	–	36.1	–
13	24.9	17.5	–	28.1	–
14	44.5	–	13.2	16.1	–
15	44.4	86.6	–	2.7	1.9
16	22.4	17.1	–	16.7	5.8
17	–	–	4.7	30.9	5.2
18	–	–	3.4	10.7	7.1
19	22.8	–	2.6	–	–
20	7	–	–	–	28.5
21	–	3.4	–	26.5	8.9
22	32.2	–	21.2	–	–
CP-55,940	91.49	103.34	–	–	–
Naloxone	–	–	99.11	101.43	101.92

Table 4

The interaction data of compounds **4**, **11**, and **15** compared to CP-55,940

Compounds	Energy	Binding pocket residues (location)						
		Lys109 TM3	Lys279 TM3	Ser285 TM7	Ser268 TM6	Ala282 TM7	Asp189 Loop2nd-Ex	
		Hydrogen bonding interaction (distance Å)						Hydrophobic interaction
CP-55,940	12	2.2	–	1.9	–	2.5	–	Val251, Met265, Leu254
4	12.5	–	3.1	3.4	–	–	–	Phe197, Val251, Phe87, Ala282
11	11.9	–	–	3.5	3.5	1.85	–	Val251, Phe197
15	13.5	2.7	3.1	–	–	–	3	Phe91, Phe283, Ala282

All interaction data are presented in the table showing the contact between the essential compounds and the residues in pocket compared to reference ligand (CP-55,940). These data includes binding energy, distance in case of hydrogen bonding interaction and amino acid residues responsible in hydrophobic contact with showing of transmembrane positions

Table 5

Molecular properties of the active compounds

Compounds	Molecular weight	Log S	TPSA	Log P(o/w)	VSA
4	499	−10.46	35.53	8.41	523.7
11	515	−9.74	55.76	7.34	533.3
15	429	−10.53	34.14	7.17	500.4
CP-55,940	377	−6.67	60.69	6.34	461.2

Different molecular descriptors were calculated including their molecular weight, solubility, polar surface area, partition coefficient, and Van Der Waals surface area